[Epub Sep 2014] ahead of print

Endo Y, Furuta A, Nishino I: Danon disease: a phenotypic expression of LAMP-2 deficiency. Acta Neuropathol. 129(3): 391-398, Mar, 2015 [Epub Jan 2015]

Tanboon J, Hayashi YK, Nishino I, Sangruchi T: Kyphoscoliosis and easy fatigability in a 14-year-old boy. Neuropathology. 35(1): 91-93, Feb 2015 [Epub Aug 2014]

Dong M, Noguchi S, Endo Y, Hayashi YK, Yoshida S, Nonaka I, Nishino I: *DAG1* mutations associated with asymptomatic hyperCKemia and hypoglycosylation of α-dystroglycan. Neurology. 84(3): 273-279, Jan, 2015 [Epub Dec 2014]

Yonekawa T, Malicdan MC, Cho A, Hayashi YK, Nonaka I, Mine T, Yamamoto T, Nishino I, Noguchi S: Sialyllactose ameliorates myopathic phenotypes in symptomatic GNE myopathy model mice. Brain. 137(10): 2670-2679, Oct, 2014 [Epub Jul 2014]

Anada RP, Wong KT, Malicdan MC, Goh KJ, Hayashi YK, Nishino I, Noguchi S: Absence of beta-amyloid deposition in the central nervous system of a transgenic mouse model of distal myopathy with rimmed vacuoles. Amyloid. 21(2): 138-139, Jun, 2014 [Epub Mar 2014]

Cho A, Hayashi YK, Monma K, Oya Y, Noguchi S, Nonaka I, Nishino I: Mutation profile of the *GNE* gene in Japanese patients with distal myopathy with rimmed vacuoles (GNE myopathy). J Neurol Neurosurg Psychiatry. 85(8): 912-915, Aug, 2014

Kajino S, Ishihara K, Goto K, Ishigaki K, Noguchi S, Nonaka I, Osawa M, Nishino I, Hayashi YK: Congenital fiber type disproportion myopathy caused by LMNA mutations. J Neurol Sci. 340(1-2): 94-98, May, 2014 [Epub Mar 2014]

Mori-Yoshimura M, Oya Y, Yajima H, Yonemoto N, Kobayashi Y, Hayashi YK, Noguchi S, Nishino I, Murata M: GNE myopathy: A prospective natural history study of disease progression. Neuromuscul Disord. 24(5): 380-386, May, 2014 [Epub Feb 2014]

Goto M, Okada M, Komaki H, Sugai K, Sasaki M, Noguchi S, Nonaka I, Nishino I, Hayashi YK: A nationwide survey on marinesco-sjogren syndrome in Japan. Orphanet J Rare Dis. 9(1): 58, Apr, 2014.

米川貴博，西野一三：縁取り空胞を伴う遠位型ミオパチー．Clinical Neuroscience 臨床神経科学．33(3): 348-349, Mar, 2015

2. 学会発表

Nishino I: Progress in therapy for GNE myopathy. The 4th Oriental Congress of

Neurology, Shanghai, China,(Shanghai International Convention Center), 3.27, 2015(3.25-3.28)

Nishino I: Treatment of GNE myopathy. 14th AOMC ANNUAL SCIENTIFIC MEETING 2015 (AOMC), Bangkok, Thailand,(Shangri-La Hotel), 3.3, 2015(3.1-3.4)

Nishino I: GNE MYOPATHY – WILL IT BE TREATABLE? Brain Conference 2014 Joint Conference of the KSBNS (The Korean Society of Brain and Neural Science), CASN (The 3rd Congress of Asian Society of Neuropathology) and KSND (The Korean Society for Neurodegenerative Disease), Seoul, Korea, (Seoul National University), 11.6, 2014

Nishino I: Introduction to clinical features of GNE myopathy. GNE myopathy Consortium Workshop, Berlin, Germany, (BEUTH HOCHSCHULE FUR TECHNIK BERLIN University of Applied Sciences), 10.12, 2014

Nishimura H, Suzuki S, Uruha A, Noguchi S, Hayashi YK, Mitsuhashi S, Nonaka I, Nishino I: Positivity for anti-cytosolic 5'-nucleotidase 1A autoantibody in inflammatory myopathies. 19th International Congress of the World Muscle Society, Berlin, Germany (Langenbeck-Virchow-Haus), 10.8, 2014 (10.7-10.11)

Nishino I: Therapeutic interventions in GNE-myopathy and possible targets in myofibrillar myopathies. 13th INTERNATIONAL CONGRESS ON NEUROMUSCULAR DISEASES, Nice, France (Nice Acropolis Convention Center), 7.7, 2014(7.5-7.10)

Nishino I: Therapy of DMRV/hIBM (GNE) myopathies. 13th INTERNATIONAL CONGRESS ON NEUROMUSCULAR DISEASES, Nice, France (Nice Acropolis Convention Center), 7.7, 2014(7.5-7.10)

その他（講演等）

西野一三：海外での治験．遠位型ミオパチー市民公開講座－治療法開発を目指して－，小平市(国立精神・神経医療研究センター), 11.1, 2014, 主催:厚生労働科学研究費補助金 難治性疾患等政策研究事業(難治性疾患政策研究事業)「希少難治性筋疾患に関する調査研究(H26-難治等(難)・一般-079)」班　研究代表者 青木正志(東北大学), 厚生労働科学研究費補助金 難治性疾患等実用化研究事業(難治性疾患実用化研究事業)「遠位型ミオパチーにおけるN-アセチルノイラミン酸の薬物動態の検討及び2/3相試験(H25-難治等(難)-一般-026)」班　研究代表者 青木正志，厚生労働科学研究補助金 障害者対策総合研究事業(障害者対策総合研究開発事業(神経・筋疾患分野))「縁取り空胞を伴う遠位型ミオパチーに対するさらに高い効果の期待される治療薬の開発(H25-神経・筋-一般-004)」班　研究代表者 野口　悟(国立精神・神経医療研究センター), NPO法人 PADM遠位型ミオパチー患者会

H. 知的財産権の出願・登録状況

（予定を含む）

1. 特許申請

発明の名称：GNE タンパク質の機能低下に起因する疾患の治療用医薬剤、食品組成物、食品添加物

発明者名：

野口　悟，Malicdan MC，西野一三

権利者名：

公益財団法人ヒューマンサイエンス振興財団

出願番号：特願 2011-513374

登録番号：第 5626734 号

登録日　：平成 26(2014)年 10 月 10 日

発明の名称：GNE タンパク質の機能低下に起因する疾患の治療用医薬剤、食品組成物

特許権者：

公益財団法人ヒューマンサイエンス振興財団

発明者　：

野口　悟，Malicdan MC，西野一三

国名：中国 (PCT/JP2010/058116)

出願番号：201080021386.4

基礎出願番号：特願 2009-119272

登録番号：ZL201080021386.4

登録日　：平成 27(2015)年 2 月 11 日

2. 実用新案登録

特になし

3. その他

特になし

III.　研究成果の刊行に関する一覧表

研究成果の刊行に関する一覧表

発表者氏名：論文タイトル名．発表誌名 巻号：ページ，出版年
Uruha A, Hayashi YK, Oya Y, Mori-Yoshimura M, Kanai M, Murata M, Kawamura M, Ogata K, Matsumura T, Suzuki S, Takahashi Y, Kondo T, Kawarabayashi T, Ishii Y, Kokubun N, Yokoi S, Yasuda R, Kira JI, Mitsuhashi S, Noguchi S, Nonaka I, Nishino I: Necklace cytoplasmic bodies in hereditary myopathy with early respiratory failure. ***J Neurol Neurosurg Psychiatry.*** [Epub Sep 2014] ahead of print
Endo Y, Furuta A, Nishino I: Danon disease: a phenotypic expression of LAMP-2 deficiency. ***Acta Neuropathol.*** 129(3): 391-398, Mar, 2015 [Epub Jan 2015]
Tanboon J, Hayashi YK, Nishino I, Sangruchi T: Kyphoscoliosis and easy fatigability in a 14-year-old boy. ***Neuropathology.*** 35(1): 91-93, Feb 2015 [Epub Aug 2014]
Dong M, Noguchi S, Endo Y, Hayashi YK, Yoshida S, Nonaka I, Nishino I: *DAG1* mutations associated with asymptomatic hyperCKemia and hypoglycosylation of α-dystroglycan. ***Neurology.*** 84(3): 273-279, Jan, 2015 [Epub Dec 2014]
Yonekawa T, Malicdan MC, Cho A, Hayashi YK, Nonaka I, Mine T, Yamamoto T, Nishino I, Noguchi S: Sialyllactose ameliorates myopathic phenotypes in symptomatic GNE myopathy model mice. ***Brain.*** 137(10): 2670-2679, Oct, 2014 [Epub Jul 2014]
Anada RP, Wong KT, Malicdan MC, Goh KJ, Hayashi YK, Nishino I, Noguchi S: Absence of beta-amyloid deposition in the central nervous system of a transgenic mouse model of distal myopathy with rimmed vacuoles. ***Amyloid.*** 21(2): 138-139, Jun, 2014 [Epub Mar 2014]

Cho A, Hayashi YK, Monma K, Oya Y, Noguchi S, Nonaka I, Nishino I: Mutation profile of the *GNE* gene in Japanese patients with distal myopathy with rimmed vacuoles (GNE myopathy). ***J Neurol Neurosurg Psychiatry.*** 85(8): 912-915, Aug, 2014
Kajino S, Ishihara K, Goto K, Ishigaki K, Noguchi S, Nonaka I, Osawa M, Nishino I, Hayashi YK: Congenital fiber type disproportion myopathy caused by LMNA mutations. ***J Neurol Sci.*** 340(1-2): 94-98, May, 2014 [Epub Mar 2014]
Mori-Yoshimura M, Oya Y, Yajima H, Yonemoto N, Kobayashi Y, Hayashi YK, Noguchi S, Nishino I, Murata M: GNE myopathy: A prospective natural history study of disease progression. ***Neuromuscul Disord.*** 24(5): 380-386, May, 2014 [Epub Feb 2014]
Goto M, Okada M, Komaki H, Sugai K, Sasaki M, Noguchi S, Nonaka I, Nishino I, Hayashi YK: A nationwide survey on marinesco-sjogren syndrome in Japan. ***Orphanet J Rare Dis.*** 9(1): 58, Apr, 2014.

IV.　研究成果の刊行物・別刷

JNNP Online First, published on September 24, 2014 as 10.1136/jnnp-2014-309009

RESEARCH PAPER

Necklace cytoplasmic bodies in hereditary myopathy with early respiratory failure

Akinori Uruha,[1,2,3] Yukiko K Hayashi,[1,2,4] Yasushi Oya,[5] Madoka Mori-Yoshimura,[5] Masahiro Kanai,[5] Miho Murata,[5] Mayumi Kawamura,[6] Katsuhisa Ogata,[7] Tsuyoshi Matsumura,[8] Shigeaki Suzuki,[9] Yukako Takahashi,[10,11] Takayuki Kondo,[11] Takeshi Kawarabayashi,[12] Yuko Ishii,[13] Norito Kokubun,[13] Satoshi Yokoi,[14] Rei Yasuda,[15] Jun-ichi Kira,[16] Satomi Mitsuhashi,[1,2] Satoru Noguchi,[1,2] Ikuya Nonaka,[2,7] Ichizo Nishino[1,2]

▶ Additional material is published online only. To view please visit the journal online (http://dx.doi.org/10.1136/jnnp-2014-309009).

For numbered affiliations see end of article.

Correspondence to
Dr Ichizo Nishino, Department of Neuromuscular Research, National Institute of Neuroscience, NCNP, 4-1-1 Ogawa-Higashi, Kodaira, Tokyo 187-8502, Japan; nishino@ncnp.go.jp

Received 15 July 2014
Revised 2 September 2014
Accepted 7 September 2014

ABSTRACT

Background In hereditary myopathy with early respiratory failure (HMERF), cytoplasmic bodies (CBs) are often localised in subsarcolemmal regions, with necklace-like alignment (necklace CBs), in muscle fibres although their sensitivity and specificity are unknown.

Objective To elucidate the diagnostic value of the necklace CBs in the pathological diagnosis of HMERF among myofibrillar myopathies (MFMs).

Methods We sequenced the exon 343 of *TTN* gene (based on ENST00000589042), which encodes the fibronectin-3 (FN3) 119 domain of the A-band and is a mutational hot spot for HMERF, in genomic DNA from 187 patients from 175 unrelated families who were pathologically diagnosed as MFM. We assessed the sensitivity and specificity of the necklace CBs for HMERF by re-evaluating the muscle pathology of our patients with MFM.

Results *TTN* mutations were identified in 17 patients from 14 families, whose phenotypes were consistent with HMERF. Among them, 14 patients had necklace CBs. In contrast, none of other patients with MFM had necklace CBs except for one patient with reducing body myopathy. The sensitivity and specificity were 82% and 99%, respectively. Positive predictive value was 93% in the MFM cohort.

Conclusions The necklace CB is a useful diagnostic marker for HMERF. When muscle pathology shows necklace CBs, sequencing the FN3 119 domain of A-band in *TTN* should be considered.

INTRODUCTION

Hereditary myopathy with early respiratory failure (HMERF; OMIM 603689) is an adult-onset progressive myopathy characterised by early presentation of respiratory insufficiency usually during ambulant stage.[1–3] Pathologically, HMERF shares features of myofibrillar myopathy (MFM) besides the key finding of cytoplasmic bodies (CBs).[2 3] Its causative gene *TTN*, which encodes a gigantic protein, titin,[2 3] is known to be causative also for tibial muscular dystrophy, limb girdle muscular dystrophy type 2J, early-onset myopathy with fatal cardiomyopathy and dilated or hypertrophic cardiomyopathy.[4–10] Interestingly, all patients with HMERF so far identified carry a mutation in exon 343 (based on ENST00000589042) encoding the fibronectin-3 (FN3) 119 domain in the A-band region of titin.[2 3 11–17]

CBs are abnormal protein aggregates visualised usually as red-colored objects on modified Gomori trichrome stain and can be observed in a wide range of myopathic conditions. Nevertheless, they are often conspicuous in MFM and considered as one of the representative pathological findings in MFM.[18] In muscle specimens of HMERF, CBs are often located in the subsarcolemmal region,[12 13 14 19] with a necklace-like alignment, which here we call 'necklace CBs'. However, the utility of necklace CBs in the pathological diagnosis of HMERF is unknown. We therefore tested the sensitivity and specificity of necklace CBs in the diagnosis of HMERF.

METHODS

Patients

National Center of Neurology and Psychiatry (NCNP) functions as a referral centre for muscle pathology and muscle biopsy samples are sent from all over Japan. From 1991 to 2013, 187 patients from unrelated 175 Japanese families have been pathologically diagnosed as MFM at NCNP. In this cohort, mutations were found in known MFM-related genes: *DES*: 8 families (4.6%), *VCP*: 8 families (4.6%), *FLNC*: 6 families (3.4%), *DNAJB6*: 6 families (3.4%), *ZASP*: 5 families (2.9%), *FHL1*: 5 families (2.9%), *MYOT*: 4 families (2.3%) and *BAG3*: 1 family (0.6%). No mutation was identified in *CRYAB*. Clinical information at the time of muscle biopsy was available in all patients.

Genetic analysis

Genomic DNA was isolated from peripheral lymphocytes or frozen muscle as previously described.[20] Exon 343 of *TTN* was directly sequenced using ABI PRISM 3130 automated sequencer (PE Applied Biosystems). Sequence variants were assessed using publically available databases including 1000 Genomes Project database (http://www.1000genomes.org/), NHLBI Exome Sequencing Project 5400 database (http://evs.gs.washington.edu/EVS/), dbSNP135 (http://www.ncbi.nlm.nih.gov/SNP/) and Human Genetic Variation Browser (http://www.genome.med.kyoto-u.ac.jp/SnpDB/); and

To cite: Uruha A, Hayashi YK, Oya Y, *et al*. *J Neurol Neurosurg Psychiatry* Published Online First: [*please include* Day Month Year] doi:10.1136/jnnp-2014-309009

Table 1 Clinical features of the patients with *TTN* variants

Patient Number	Age (years)/ sex	Relationship	Mutation (protein level)	Family history (years)	Initial manifestations (years)	Age at gait disturbance/ ambulant	Foot drop (years)	Respiratory disturbance (years)	Artificial ventilation (years)	Cardiac involve-ment	Dysphagia (years)	Other features
A-1	49/M	Father	p.C31712R		Tripping (46)	46/yes	Yes (NA)	Yes (48)	Yes (49)	RHF	No	No
A-2	26/M	Son			Tripping (20)	22/yes	Yes (22)	Yes*	No	No	No	No
B-1	45/M	Older brother	p.C31712R	Father: Foot drop; sudden death (42) Oldest brother: gait disturbance (32); sudden death (40)	Foot drop (31)	31/yes	Yes (31)	Yes (44)	Yes (45)	No	No	No
B-2	37/M	Younger brother			Foot drop (27)	27/yes	Yes (27)	Yes (34)	Yes (37)	No	No	No
C	34/F		p.C31712R		Fatiguability (26)	29/yes	Yes (31)	Yes (26)	Yes (31)	–	No	Difficulty in opening mouth
D	38/M		p.C31712R		Difficulty in lifting thigh (20)	20/no (32)	Yes (20 s)	Yes (29)	Yes (29)	STC	Yes (28) Artificial nutrition (35)	
E	40/M		p.C31712R	Mother: sudden death (38) Older sister: proximal muscle weakness; respiratory failure (35)	Fatiguability; respiratory failure (31)	31/yes	Yes (NA)	Yes (31)	Yes (37)	RHF, PH	–	
F	52/M		p.C31712R		Foot drop (47)	47/yes	Yes (47)	Yes (50)	Yes (52)	–	Yes (47)	
G-1	58/M	Father	p.C31712R	Grandfather of G-2: died of respiratory failure (45)	Tripping (57)	57/yes	Yes (58)	Yes*	–	–	–	
G-2	29/M	Son			Tripping (20)	20/yes	Yes (20 s)	Yes (29)	Yes (29)	RHF	–	
H	68/F		p.C31712R	Son: distal myopathy; sudden death	Difficulty in standing on right toe (56)	56/yes	No	Yes (68)	Yes (68)	RHF, Af	–	Head drop; forward bent posture
I	43/M		p.C31712R		Fatiguability; weight loss (39)	42/yes	No	Yes (39)	Yes (42)	–	Yes (42)	Myalgia muscle cramp
J	42/F		p.C31712Y		Difficulty lifting thighs (36)	38/Yes	No	Yes*	–	–	–	
K	38/M		p.G31791D		Gait disturbance (28)	28/Yes	Yes (30)	Yes*	Yes (38)	–	Yes (36)	Head drop
L	44/F		p.G31791R		Fatiguability; loss of appetite (40)	41/yes	No	Yes (40)	Yes (44)	STC	–	
M	40/M		p.G31791V	Mother and younger sister: lower leg muscle weakness	Gait disturbance (24)	24/yes	Yes (27)	Yes*	–	2° AVB (type 1)	–	
N	46/M		p.R31783_V31785del		Foot drop; difficulty in opening a bottle (41)	41/yes	Yes (41)	Yes*	–	–	–	Myalgia

*Asymptomatic but found by laboratory tests.
2° AVB (type 1), Mobitz type 1 second degree atrioventricular block; Af, atrial fibrillation; F, female; M, male; NA, not available; PH, pulmonary hypertension; RHF, right-sided heart failure; STC, sinus tachycardia.

softwares to predict functional effects of mutations such as PolyPhen-2 (http://genetics.bwh.harvard.edu/pph2/) and Mutation Taster (http://www.mutationtaster.org/). The description of mutations of *TTN* conforms to Ensemble sequence ENST00000589042.

In this study a diagnosis of HMERF was made based on the presence of a mutation in exon 343 of *TTN*, although the possibility that mutations in other parts of the gene cause HMERF cannot be totally excluded.

Re-evaluation of muscle pathology

Muscle pathology was re-evaluated focusing on necklace CBs on modified Gomori trichrome. In the present study, we tentatively defined the presence of necklace CBs as at least two muscle fibres containing CBs exclusively localised in the subsarcolemmal area, covering more than 50% of circumference of each muscle fibre in three non-serial sections (each section was at least 250 μm apart and included at least 300 muscle fibres). CBs were evaluated in all MFM cases, and subsequently the sensitivity and specificity of necklace CBs for the diagnosis of HMERF were calculated. The positive predictive value (PPV) and 95% CIs were calculated with GraphPad Prism V.5.0 (Graph Pad Software, California, USA).

Electron microscopic observation

Biopsied muscle specimens were fixed in 2.5% glutaraldehyde and post-fixed with 2% osmium tetroxide. Semithin sections stained with toluidine blue were examined by light microscopy. Ultrastructural analysis was carried out on longitudinal and transverse ultrathin sections of muscles after staining with uranyl acetate and lead citrate, using Tecnai spirit transmission electron microscope (FEI, Hillsboro, Oregon, USA).

Re-evaluation of clinical data

The clinical information in our cohort together with previous reports[2 3 11–14] showed that respiratory insufficiency before being wheelchair users and selective involvement of semitendinosus muscles on muscle imaging were frequently observed, raising a possibility that these findings might be clues for the diagnosis of HMERF. We therefore reviewed clinical data of our patients with MFM in order to calculate sensitivities, specificities and PPVs of them at the time of muscle biopsy.

Ethics

All of the clinical information and materials used in this study were obtained for diagnostic purpose and permitted for scientific use with written informed consent. All experiments in this study were approved by the Ethical Committee of National Center of Neurology and Psychiatry.

RESULTS

Mutation analysis

Six different heterozygous mutations in exon 343 of *TTN* were identified in 17 patients from 14 families (table 1). Among them, two mutations, g.284701T>C (c.95134T>C; p.C31712R) and g.284939G>A (c.95372G>A; p.G31791D) were previously reported.[2 3 11 12 14] The former mutation was reported to be the most common in other populations.[11 12] This was also the case in our cohort and the mutation was shared by nine families, while all others were found in single families. The latter mutation was previously reported in a European-American family.[14] Among four novel mutations that we identified, three were missense: g.284702G>A (c.95135G>A; p.C31712Y), g.284938G>C (c.95371G>C; p.G31791R) and g.284939G>T (c.95372G>T; p.G31791V); and one was non-frameshift deletion: g.284913_284921delGAGGGCAGT (c.95346_95354del; p.R31783_V31785del). None of the variants was listed in the

Table 2 Laboratory findings at the time of muscle biopsy

Patient	CK IU/L (normal value)	Respiratory function (%VC, sitting position)	Selective involvement of muscles on imaging test: Semitendinosus muscle	Selective involvement of muscles on imaging test: Anterior compartment of lower legs	Muscle pathology: CB	Muscle pathology: Necklaces of CBs	Muscle pathology: RV
A-1 (49 years)	Normal (value: NA)	Abnormal (value: NA.)	NA	NA	+	+	+
A-2 (26 years)	65 (20–190)	77% (68%, lying)	+	+	+	+	+
B-1 (39 years)	425 (51–197)	84% → 67% (45 years)	+	+	+	+	−
B-2 (32 years)	659 (–200)	82% → 63% (37 years)	+	+	+	+	+
C (31 years)	488 (45–170)	32%	NA (+, 34 years)	NA (+, 34 years)	+	+	−
D (31 years)	375 (51–197)	VC: 0.97 L	+	−*	+	+	−
E (40 years)	234 (62–287)	ABG: $PaCO_2$ 86 mm Hg, PaO_2 56 mm Hg (RA)	+	+	+	+	−
F (50 years)	61 (NA)	41%	+	+	+	−	−
G-1 (58 years)	146 (50–170)	59%	+	+	+	−	−
G-2 (29 years)	142 (50–170)	31%	+	+	+	+	+
H (68 years)	140 (50–170)	ABG: PaCO2 60 mm Hg	+	+	+	+	−
I (43 years)	179 (62–287)	40%	+	+	+	−	−
J (42 years)	364 (45–163)	64%	+	+	+	+	+
K (34 years)	645 (51–197)	67% (55%, lying)	+	+	+	+	+
L (44 years)	139 (43–165)	36%	+	+	+	+	−
M (40 years)	190 (62–287)	61%	−*	+	+	+	+
N (46 years)	799 (62–287)	67%	+	+	+	+	+

In the column of Patient, the same alphabet indicates that they belong to the same family.
*Diffuse muscle involvement.
ABG, arterial blood gas; CB, cytoplasmic body; NA, not available; RV, rimmed vacuole; VC, vital capacity.

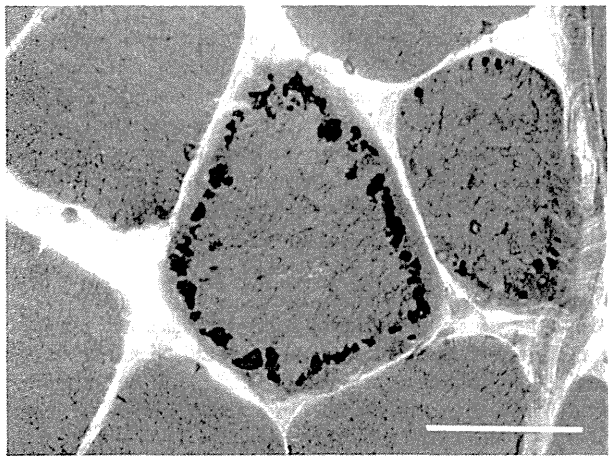

Figure 1 Necklace cytoplasmic bodies. Cytoplasmic bodies are located in line in subsarcolemmal region, often covering the total circumference of a muscle fibre. Modified Gomori trichrome stain. Bar: 50 μm.

genomic variation databases. The mutated amino acids were highly conserved among species (UCSC Genome Browser). PolyPhen-2 predicted p.C31712Y, p.G31791R and p.G31791V mutations as probably damaging with scores 0.996, 1.000 and 1.000, respectively. Likewise, Mutation Taster predicted the p.C31712Y, p.G31791R, p.G31791V and p.V31782_A31784del mutations to be disease-causing with a probability of 1.000, 1.000, 1.000 and 0.998, respectively. No segregation analysis was possible in any family.

Clinical information of 17 participants with *TTN* mutations are summarised in tables 1 and 2 and online supplementary table. All patients show clinical signs consistent with HMERF previously reported.[1–3 11–14] The median age of onset was 31 years (range 20–57 years). Four patients developed dysphagia, and one of them required tube feeding.

Table 3 Cross tabulation of necklace cytoplasmic bodies and hereditary myopathy with early respiratory failure

	Patients with myofibrillar myopathies		
Necklace CBs	HMERF	Non-HMERF	Row total
+	14	1	15
% within column	82.4%	0.6%	
% within row	93.3%	6.7%	
–	3	169	172
% within column	17.6%	99.4%	
% within row	1.7%	98.3%	
Column total	17	170	187

CB, cytoplasmic body; HMERF, hereditary myopathy with early respiratory failure.

Sensitivity and specificity of the necklace of CBs

Among 17 genetically-confirmed patients with HMERF, necklace CBs were found in 14 patients, comprising 0.1–0.8% of the muscle fibres (figure 1). In contrast, none of the 170 patients who had MFM other than HMERF had necklace CBs except for only one patient who had reducing body myopathy, which had been confirmed by the presence of reducing bodies in muscle fibres on menadione-linked α-glycerophosphate dehydrogenase (MAG) stain without substrate and a mutation in the second LIM domain of *FHL1* (g.60438G>A; c.377G>A; p.C126Y, based on ENST00000543669; online supplementary figure S1). Based on these results, the sensitivity and specificity of the necklace CBs in HMERF were calculated as 82% (14/ 17, 95% CI 57% to 96%) and 99% (169/170, 95% CI 97% to 100%), respectively (table 3). Since the prevalence of HMERF in the MFM cohort was 9.1% (17/ 187), the PPV was calculated as 93% (95% CI 68% to 100%) based on Bayes' theorem.

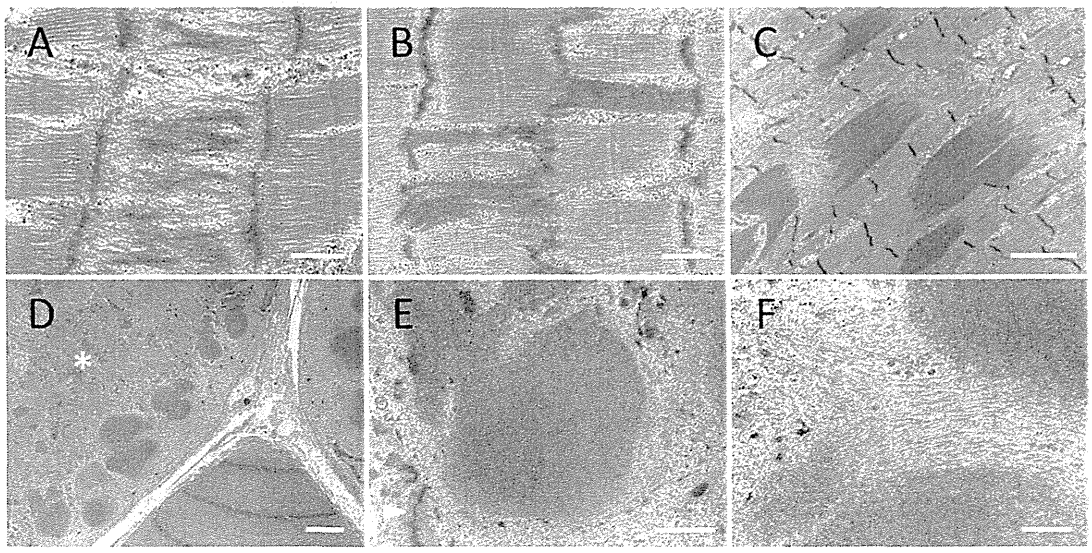

Figure 2 Electron microscope images. (A and B) Sarcomeric disarrangement limited to one sarcomere is observed. (C) Multiple electron-dense inclusions are present in association with Z lines. (D) A fibre containing necklace cytoplasmic bodies (CBs) shows marked myofibrillar disorganisation (asterisk), especially around the CBs. (E) CBs showing a necklace alignment with lower electron density as compared to that of Z line. △: a remnant of Z line. (F) Thin filamentous structure around the CBs. Lattice-like structure is not seen in the CBs. Bar: 0.5 μm (A, B and F), 1 μm (E), 2 μm (C), and 5 μm (D).

Muscle specimens of the three patients with HMERF had CBs, which are usually located in the subsarcolemmal regions, but did not show the definite necklace-like alignment pattern (online supplementary figure S2). Those three patients shared the same mutation, g.284701T>C (p.C31712R), albeit other nine patients harbouring the same mutation had definite necklace CBs.

Fibres with rimmed vacuoles were occasionally seen, but the sensitivity, specificity and PPV for HMERF were lower than those of the necklace CBs: 47% (8/ 17, 95% CI 23% to 72%), 61% (104/ 170, 95% CI 53% to 69%) and 11% (95% CI 20% to 48%), respectively.

Ultrastructural features

EM samples were available from four patients with HMERF. Sarcomeric disarrangement limited to one sarcomere was observed in all patients (figure 2A, B). In some areas, multiple electron-dense inclusions associated with Z line were surrounded by disorganised myofibrils (figure 2C). Fibres with necklace CBs were included only in one sample. These fibres showed marked myofibrillar disorganisation (figure 2D, asterisk), especially in the vicinity of the CBs (figure 2D, E). The CBs had a lower electron density as compared with that of the Z line and contained dense and mildly filamentous components, without lattice-like structure (figure 2E, F). Small number of CBs were partly surrounded by thin filaments (figure 2F).

Sensitivity and specificity of respiratory dysfunction and muscle imaging data

Using the data at the time of muscle biopsy about the respiratory function of 102 participants in the MFM cohort, the sensitivity, specificity and PPV of the respiratory insufficiency before being wheelchair users (below 80% of vital capacity or over 45 mm Hg of $PaCO_2$) were calculated as 88% (14/16, 95% CI 62% to 99%), 94% (81/86, 95% CI 87% to 98%) and 74% (95% CI 49% to 91%), respectively (table 2 and 4). In five non-HMERF participants presenting respiratory insufficiency during the ambulant stage, one had a mutation in *VCP*, but no causative genes were identified in four participants as far as we have screened.

As for the muscle imaging at the time of muscle biopsy, the sensitivity of selective muscle involvement of semitendinosus muscles as shown in figure 3 was 93% (14/ 15; table 4). The specificity could not be calculated due to the limited number of images available in non-HMERF participants.

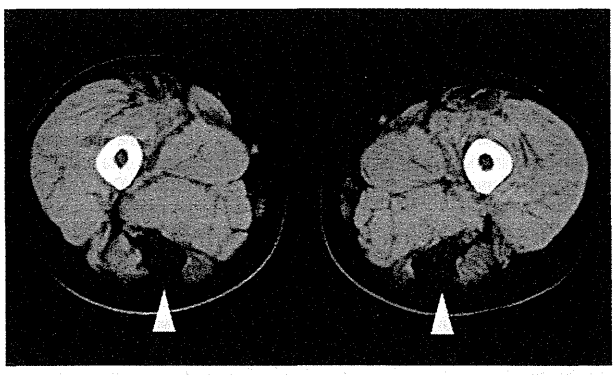

Figure 3 Muscle image. Representative image showing preferential involvement of semitendinosus muscles. CT images of skeletal muscles in proximal legs of the patient K. △: semitendinosus muscles.

DISCUSSION

We have demonstrated that necklace CBs had high specificity for a diagnosis of HMERF (99%), with sensitivity 82% and PPV 93% in our MFM cohort. In this study, all 15 patients with necklace CBs had HMERF except for only one who had reducing body myopathy due to a mutation in *FHL1*, without mutation in exon 343 of *TTN*. Although we judged this case as having necklace CBs retrospectively, CBs in this case are smaller in size and scattered in the subsarcolemmal region in muscle fibres, giving an appearance different from typical necklace CBs in HMERF (online supplementary figure S1), suggesting that the specificity of necklace CBs could be substantially 100%. In addition, muscle pathology of this patient showed typical reducing bodies in scattered fibres on MAG stain without substrate, and thus differential diagnosis between reducing body myopathy and HMERF was not a problem in practise.

Interestingly, even in three patients with HMERF without typical necklace CBs, CBs are aligned in the subsarcolemmal regions in muscle fibres, albeit they do not encompass more than half of the myofibre circumference (online supplementary figure S2), suggesting that this unique subsarcolemmal alignment pattern is likely to be related to the dysfunction of titin due to exon 343 mutations although the detailed mechanism is still unknown.

On electron microscopy (EM), CBs in the patients differ slightly from typical CBs seen in other various diseases. While typical CBs consists of a core with electron density similar to Z line,[21] the CBs in HMERF show lower density. Furthermore, thin filaments, which compose a halo of typical CBs, are rarely seen around the CBs. Interestingly, the sarcomeric disarrangement appears to progress in order of figure 2A, C, suggesting a possibility that this sarcomeric disarrangement may ultimately produce the CBs.

Several groups reported that CBs in HMREF are reactive to antibodies to myofibrillar proteins including myotilin, αB-crystallin, actin (phalloidin), filamin C, dystrophin, and γ-sarcoglycan, but not for titin on immunohistochemical analysis.[11 12 14 19] Although similar findings were obtained in our observation (data not shown), the pathophysiological significance of CBs in HMERF has still not been elucidated.

We found four novel variants in exon 343 of *TTN* including three heterozygous missense mutations [g.284702G>A (p.C31712Y), g.284938G>C (p.G31791R) and g.284939G>T (p.G31791V)], and a heterozygous deletion variant [g.284913_284921del (p.R31783_V31785del)]. These variants were not described in any of the publically available databases. Mutated amino acids are highly conserved among species. Also

Table 4 Sensitivity, specificity, and positive predictive value of laboratory findings for HMERF

	Respiratory disturbance in the ambulant stage	Selective affected semitendinosus muscles on muscle imaging	Necklace CBs on muscle pathology
Sensitivity	88% (14/16)	93% (14/15)	82% (14/17)
Specificity	94% (81/86)	NA	99% (169/170)
PPV	74%	NA	93%

At the time of muscle biopsy.
Respiratory disturbance: <80% of %VC or >45 mm Hg of $PaCO_2$. PPVs were calculated by the HMERF prevalence of 9.1% in the MFM cohort.
CB, cytoplasmic body; HMERF, hereditary myopathy with early respiratory failure; MFM, myofibrillar myopathy; NA, not available, PPV, positive predictive value; VC, vital capacity.

Table 5 Mutations in the FN3 119 domain of A-band in *TTN* in HMERF

DNA change	Amino acid change	Origin	Family	Reference
g.284693C>G	p.P31709R (p.P30068R)	French		3
g.284701T>C	p.C31712R (p.C30071R)	Swedish, British, Finnish, Italian, Spanish, Argentinian (European ancestry), East Indian, Japanese	A, B, C, D, E, F, G, H, I	2, 3, 11, 12, 14
g.284702G>A	p.C31712Y (p.C30071Y)	Japanese	J	*
g.284752T>C	p.W31729R (p.W30088R)	British		12
g.284754G>C	p.W31729C (p.W30088C)	German		12
g.284753G>T	p.W31729L (p.W30088L)	Japanese		13
g.284762C>T	p.P31732L (p.P30091 L)	Italian, French, British, Portuguese, Swedish		11, 12, 15, 16, 17
g.284913_284921del	p.R31783_V31785del (p.R30142_V30144del)	Japanese	N	*
g.284925C>G	p.N31786K (p.N30145 K)	British		11
g.284939G>A	p.G31791D (p.G30150D)	American (European ancestry), Japanese	K	14
g.284938G>C	p.G31791R (p.G30150R)	Japanese	L	*
g.284939G>T	p.G31791V (p.G30150V)	Japanese	M	*

*Possible novel mutation. Titin reference: ENST00000589042 and ENST00000591111, a former transcript, inside the brackets.
HMERF, hereditary myopathy with early respiratory failure.

the variants were predicted to be pathogenic by the plural prediction software programs. Furthermore, in single-base substitutions, other types of substitutions of the same amino acids (p.C31712R and p.G31791D) have already been reported in other families with HMERF (table 5).[2 3 11 12 14] Thus, although segregation analysis was not possible, the variants are highly likely to be pathogenic.

Previous reports suggested that HMERF might not be extremely rare in Caucasian populations.[11 12] In UK, in patients with HMERF with p.C31712R (p.C30071R, based on ENST00000591111), mutation in exon 343 of *TTN* was identified in 5.5% of the MFM cohort.[11] Patients have also been identified in Asian populations including Japanese and Indian, suggesting that patients with HMERF are likely to be distributed worldwide.[13 14 22] Here, we confirmed the presence of patients with HMERF in Japan. Furthermore, among all the 175 MFM families in our Japanese cohort, 14 families (8%) had HMERF with mutations in the exon 343 of *TTN*, which renders *TTN* the most frequent causative gene for MFM in our cohort although there still remains a possibility that there may be an undisclosed major causative gene as causative mutations have not been identified in more than 60% of the MFM families.

Clinical features of participants with HMERF described in this study coincide with those in previous reports for most parts: affected individuals usually present with predominant distal leg muscle weakness followed by chronic respiratory failure.[1–3 11–14] Interestingly, dysphagia was seen in 4 of the 17, which was rarely described in the literature.[13] Dysphagia seems to be mostly mild, but was severe in one patient, who required tube feeding.

Skeletal muscle imaging has been reported to show preferential involvement of semitendinosus, obturator, sartorius, gracilis, iliopsoas muscles and anterior compartment of lower legs, suggesting such imaging findings are useful for the diagnosis of HMERF.[3 11 12 19] Particularly, selective involvement of semitendinosus muscles is commonly observed. Our study showed a sensitivity of 93%, which is compatible with 95–100% reported by previous studies.[3 12] Unfortunately, skeletal muscle imaging was not available in many of our patients with MFM other than HMERF, and thus it was impossible to calculate the specificity and PPV of the selective involvement of semitendinosus muscles. However, it may not be so specific since such finding was observed also in other MFMs caused by mutations in *DES*, *CRYAB* and *MYOT*.[23 24]

In conclusion, the necklace CB is a useful pathological marker in the diagnosis of HMERF. When muscle pathology shows necklace CBs, sequencing the FN3 119 domain of the A-band in *TTN* should be considered.

Author affiliations
[1]Department of Clinical Development, Translational Medical Center, National Center of Neurology and Psychiatry (NCNP), Tokyo, Japan
[2]Department of Neuromuscular Research, National Institute of Neuroscience, NCNP, Tokyo, Japan
[3]Department of Education, Interdisciplinary Graduate School of Medicine and Engineering, University of Yamanashi, Yamanashi, Japan
[4]Department of Neurophysiology, Tokyo Medical University, Tokyo, Japan
[5]Department of Neurology, National Center Hospital, NCNP, Tokyo, Japan
[6]Department of Neurology, Japanese Red Cross Society, Wakayama Medical Center, Wakayama, Japan
[7]Institute of Clinical Research/Department of Neurology, National Hospital Organization Higashisaitama Hospital, Saitama, Japan
[8]Department of Neurology, National Hospital Organization Toneyama National Hospital, Osaka, Japan
[9]Department of Neurology, Keio University School of Medicine, Tokyo, Japan
[10]Department of Neurology, Osaka Red Cross Hospital, Osaka, Japan
[11]Department of Neurology, Graduate School of Medicine, Kyoto University, Kyoto, Japan
[12]Department of Neurology, Institute of Brain Science, Hirosaki University Graduate School of Medicine, Aomori, Japan
[13]Department of Neurology, Dokkyo Medical University, Tochigi, Japan
[14]Department of Neurology, Nagoya University Graduate School of Medicine, Nagoya, Japan
[15]Department of Neurology, National Hospital Organization Maizuru Medical Center, Kyoto, Japan
[16]Department of Neurology, Neurological Institute, Graduate School of Medical Sciences, Kyushu University, Fukuoka, Japan

Acknowledgements The authors thank Ms Kaoru Tatezawa, Ms Yoriko Kojima, Ms Kazu Iwasawa, Mr Takao Uchikai, and Ms Kanako Goto in NCNP for their technical assistance.

Contributors AU was involved in the conceptualisation and design of the study, data analysis and interpretation, literature review and drafting the manuscript. YKH was involved in the conceptualisation and design of the study, data analysis and interpretation, and manuscript revision for intellectual content. YO, MM-Y, MK, MM, MK, KO, TM, SS, YT, TK, TK, YI, NK, SY, RY, and JK were involved in the collection of clinical data. SM and SN were involved in the data interpretation (molecular data) and manuscript revision for intellectual content. IkN was involved in the supervision of pathological analysis and interpretation and manuscript revision for intellectual content. IcN was involved in the supervision of all aspects, including study design, data analysis and interpretation, and manuscript preparation.

Funding This study was supported partly by JSPS KAKENHI Grant Number of 24659437; partly by Research on Rare and Intractable Diseases, Comprehensive Research on Disability Health and Welfare and Applying Health Technology from the Ministry of Health, Labour and Welfare of Japan; and partly by Intramural Research Grant 23-5 and 26-8 for Neurological and Psychiatric Disorders of NCNP.

Competing interests None.

Ethics approval Ethical Committee of National Center of Neurology and Psychiatry.

Provenance and peer review Not commissioned; externally peer reviewed.

REFERENCES

1 Edström L, Thornell LE, Albo J, *et al*. Myopathy with respiratory failure and typical myofibrillar lesions. *J Neurol Sci* 1990;96:211–28.
2 Ohlsson M, Hedberg C, Brådvik B, *et al*. Hereditary myopathy with early respiratory failure associated with a mutation in A-band titin. *Brain* 2012;135:1682–94.
3 Pfeffer G, Elliott HR, Griffin H, *et al*. Titin mutation segregates with hereditary myopathy with early respiratory failure. *Brain* 2012;135:1695–713.
4 Haravuori H, Mäkelä-Bengs P, Udd B, *et al*. Assignment of the tibial muscular dystrophy locus to chromosome 2q31. *Am J Hum Genet* 1998;62:620–6.
5 Hackman P, Vihola A, Haravuori H, *et al*. Tibial muscular dystrophy is a titinopathy caused by mutations in TTN, the gene encoding the giant skeletal-muscle protein titin. *Am J Hum Genet* 2002;71:492–500.
6 Carmignac V, Salih MA, Quijano-Roy S, *et al*. C-terminal titin deletions cause a novel early-onset myopathy with fatal cardiomyopathy. *Ann Neurol* 2007;61:340–51.
7 Gerull B, Gramlich M, Atherton J, *et al*. Mutations of TTN, encoding the giant muscle filament titin, cause familial dilated cardiomyopathy. *Nat Genet* 2002;30:201–4.
8 Itoh-Satoh M, Hayashi T, Nishi H, *et al*. Titin mutations as the molecular basis for dilated cardiomyopathy. *Biochem Biophys Res Commun* 2002;291:385–93.
9 Herman DS, Lam L, Taylor MRG, *et al*. Truncations of titin causing dilated cardiomyopathy. *New Eng J Med* 2012;366:619–28.
10 Satoh M, Takahashi M, Sakamoto T, *et al*. Structural analysis of the titin gene in hypertrophic cardiomyopathy: identification of a novel disease gene. *Biochem Biophys Res Commun* 1999;262:411–17.
11 Pfeffer G, Barresi R, Wilson IJ, *et al*. Titin founder mutation is a common cause of myofibrillar myopathy with early respiratory failure. *J Neurol Neurosurg Psychiatry* 2014;85:331–8.
12 Palmio J, Evilä A, Chapon F, *et al*. Hereditary myopathy with early respiratory failure: occurrence in various populations. *J Neurol Neurosurg Psychiatry* 2014;85:345–53.
13 Izumi R, Niihori T, Aoki Y, *et al*. Exome sequencing identifies a novel TTN mutation in a family with hereditary myopathy with early respiratory failure. *J Hum Genet* 2013;58:259–66.
14 Toro C, Olivé M, Dalakas MC, *et al*. Exome sequencing identifies titin mutations causing hereditary myopathy with early respiratory failure (HMERF) in families of diverse ethnic origins. *BMC Neurol* 2013;13:29.
15 Vasli N, Böhm J, Le Gras S, *et al*. Next generation sequencing for molecular diagnosis of neuromuscular diseases. *Acta Neuropathol* 2012;124:273–83.
16 Hedberg C, Melberg A, Dahlbom K, *et al*. Hereditary myopathy with early respiratory failure is caused by mutations in the titin FN3 119 domain. *Brain* 2014;137(Pt 4):e270.
17 Lange S, Edström L, Udd B, *et al*. Reply: Hereditary myopathy with early respiratory failure is caused by mutations in the titin FN3 119 domain. *Brain* 2014;137(Pt 6): e279.
18 Schröder R, Schoser B. Myofibrillar Myopathies: A clinical and myopathological Guide. *Brain Pathol* 2009;19:483–92.
19 Tasca G, Mirabella M, Broccolini A, *et al*. An Italian case of hereditary myopathy with early respiratory failure (HMERF) not associated with the titin kinase domain R279W mutation. *Neuromuscul Disord* 2010;20:730–4.
20 Cho A, Hayashi YK, Momma K, *et al*. Mutation Profile of the GNE gene in Japanese patients with distal myopathy with rimmed vacuoles (GNE myopathy). *J Neurol Neurosurg Psychiatry*. 2014;85:914–17.
21 Macdonald RD, Engel AG. The cytoplasmic body: another structural anomaly of the Z disk. *Acta Neuropathol* 1969;14:99–107.
22 Uruha A, Nishino I. Think worldwide: hereditary myopathy with early respiratory failure (HMERF) may not be rare. *J Neurol Neurosurg Psychiatry* 2014;85:248.
23 Fisher D, Kley RA, Stratch K, *et al*. Distinct muscle imaging patterns in myofibrillar myopathies. *Neurology* 2008;71:758–65.
24 Wattjes MP, Kley RA, Fischer D. Neuromuscular imaging in inherited muscle diseases. *Eur Radiol* 2010;20:2447–60.

Necklace cytoplasmic bodies in hereditary myopathy with early respiratory failure

Akinori Uruha, Yukiko K Hayashi, Yasushi Oya, et al.

J Neurol Neurosurg Psychiatry published online September 24, 2014
doi: 10.1136/jnnp-2014-309009

Acta Neuropathol (2015) 129:391–398
DOI 10.1007/s00401-015-1385-4

REVIEW

Danon disease: a phenotypic expression of LAMP-2 deficiency

Yukari Endo · Akiko Furuta · Ichizo Nishino

Received: 27 October 2014 / Revised: 8 January 2015 / Accepted: 8 January 2015 / Published online: 15 January 2015

Abstract Danon disease is an X-linked disorder clinically characterized by the triad of hypertrophic cardiomyopathy, myopathy, and intellectual disability. Cardiomyopathy is a severe and life-threatening problem, for which cardiac transplantation is the only therapeutic option. The most striking finding in muscle biopsy samples is small basophilic granules scattered in myofibers, which are in fact small autophagic vacuoles surrounded by membranes with sarcolemmal features characterized by the recruitment of sarcolemmal proteins and acetylcholine esterase and by the presence of basal lamina on its luminal side. The mechanism underlying the formation of these autophagic vacuoles with unique sarcolemmal features (AVSF) still remains a mystery and its origin is unknown. In heart, cardiomyocytes show dramatically increased vacuolation and degenerative features, including myofibrillar disruption and lipofuscin accumulation. In brain, pale granular neurons and neurons with lipofuscin-like granules may be seen. Danon disease is caused by loss-of-function mutations in the *LAMP2* gene, which encodes lysosome-associated membrane protein 2 (LAMP-2), a single-spanned transmembrane protein localized in the limiting membranes of lysosomes and late endosomes. Most mutations lead to splicing defects or protein truncation, resulting in a loss of transmembrane and/or cytoplasmic domains, leading to LAMP-2 protein deficiency. LAMP-2 is required for the maturation of autophagosomes by fusion with lysosomes; therefore, LAMP-2 deficiency leads to a failure in macroautophagy. There are three LAMP-2 isoforms, LAMP-2A, -2B, and -2C. Clinical features of Danon disease are thought to be mediated by loss of the LAMP-2B isoform which is the major isoform expressed in muscle. It is also known that LAMP-2 plays a role in chaperone-mediated autophagy and RNA- and DNA-targeting autophagy. However, the precise pathophysiological mechanism through which LAMP-2 deficiency causes Danon disease is still not fully understood and its elucidation would promote the development of new therapies.

Keywords Lysosome · *LAMP2* · Autophagy · Autophagic vacuolar myopathy · Cardiomyopathy

Y. Endo · I. Nishino (✉)
Department of Clinical Development, Translational Medical Center, National Center of Neurology and Psychiatry (NCNP), 4-1-1 Ogawahigashi-cho, Kodaira, Tokyo 187-8551, Japan
e-mail: nishino@ncnp.go.jp

Y. Endo · I. Nishino
Department of Neuromuscular Research, National Institute of Neuroscience, National Center of Neurology and Psychiatry (NCNP), Kodaira, Tokyo, Japan

A. Furuta
Department of Cellular and Molecular Neuropathology, Graduate School of Medicine, Juntendo University, 2-1-1 Hongo, Bunkyo, Tokyo 113-8421, Japan

Introduction

In 1981, Danon et al. [4] first described two young boys presenting hypertrophic cardiomyopathy, skeletal myopathy, and intellectual disability. Their muscle biopsies showed vacuoles positive for both periodic acid–Schiff (PAS) staining and acid phosphatase activity, indicating that they were glycogen-laden lysosomes. Ultrastructural studies of muscle biopsy specimens showed abundant glycogen particles, most of which were contained within lysosomal sacs, either alone or together with cellular debris. These pathological features were characteristic of acid maltase deficiency observed in Pompe disease (glycogen

storage disease type II), although the heart and brain are typically not affected in the juvenile form of this disease. However, further biochemical studies revealed normal acid maltase activity both in the muscle and in the urine samples, excluding the diagnosis of Pompe disease. Therefore, Danon disease was originally reported as "lysosomal glycogen storage disease with normal acid maltase".

Danon disease is inherited as an X chromosome-linked dominant trait because in most familial cases, males are predominantly affected, whereas females usually have later onset and milder cardiac symptoms, and no male-to-male transmission has been reported. The affected patients have mutations in the X chromosome-located gene encoding the lysosome-associated membrane protein 2 (LAMP-2), a major lysosomal membrane protein. In 2000, loss-of-function mutations in the *LAMP2* gene and a deficiency of the LAMP-2 protein were reported in ten unrelated patients, including one of the patients described in the original case report [25]. LAMP-2-deficient mice manifested similar features, including vacuolar cardioskeletal myopathy and cardiac hypertrophy and dysfunction [34], indicating that LAMP-2 deficiency is the primary cause of Danon disease [25].

Clinical features

Danon disease is clinically characterized by the triad of hypertrophic cardiomyopathy, myopathy, and intellectual disability [4]. Because of the X-linked dominant inheritance, all the probands currently identified are males; nevertheless, women, who are heterozygous for *LAMP2* mutations, are also affected because they do develop cardiomyopathy, although later in adulthood. Birth and perinatal histories of Danon patients are unremarkable [26].

In a study that included 43 men and 39 women with confirmed Danon disease, men experienced symptom onset, were diagnosed, required heart transplantation or died earlier than women, as expected [1]. The average age for the onset of Danon disease symptoms was 12.1 ± 6.5 years in men and 28.1 ± 15 years in women. The average ages at disease diagnosis (based on skeletal or cardiac myopathy and cardiac pre-excitation) were 13.5 ± 7.0 years for men and 31.4 ± 15.4 years for women [1].

All patients develop cardiomyopathy, which is the most severe and life-threatening manifestation. In the affected men, cardiac symptoms such as exertional dyspnea are noted in their teens. Hypertrophic cardiomyopathy predominates in men, although some of them develop dilated disease [32], previously considered more prevalent in the affected women; however, recent data revealed nearly equal rates of dilated versus hypertrophic cardiomyopathy in women with Danon disease [1]. Conduction abnormalities were reported in more than 80 % of both male and female patients; however, the Wolff–Parkinson–White pattern on electrocardiograms was demonstrated by 68 % of men compared with 27 % of women [1].

In Danon disease, skeletal myopathy is usually mild; it is evident in most of the male patients (90 %), whereas only in a third of affected females. Weakness and atrophy are predominantly detected in the neck and shoulder girdle muscles, but can also be observed in the distal muscles. All male patients, even those without apparent muscle symptoms, have elevated serum levels of creatine kinase (CK), which are increased only in 63 % of female patients.

Cognitive disorders associated with Danon disease have been reported in 70–100 % of men and in approximately 50 % of women [1, 32]. In men, cognitive disabilities are predominantly mild to moderate, with infrequently observed severe intellectual disability; in women, mostly mild and nonspecific cognitive complaints were noted. Brain magnetic resonance imaging is usually normal.

The only treatment for Danon disease is cardiac transplantation. The mean ages at the transplantation are 17.9 ± 7.2 years in men and 33.7 ± 16.1 years in women. Death occurs at 19.0 ± 8.0 years in men and 34.6 ± 15.5 years in women [1].

Histological findings

Skeletal and cardiac muscles

In the patients with Danon disease, skeletal muscles demonstrate mild to moderate variation in the size of myofibers without necrotic or regenerative changes, accompanied with the appearance of scattered small basophilic granules [33] (Fig. 1). These granules demonstrate enhanced activity of lysosomal acid phosphatase, indicating the accumulation of lysosomal organelles in the myofibers of Danon patients. The lysosomal granules are surrounded with large vacuolar structures where sarcolemmal proteins such as dystrophin and its associated proteins, as well as extracellular matrix proteins and acetylcholine esterase (AChE) are recruited (Fig. 1). These lysosomal structures are known as autophagic vacuoles with unique sarcolemmal features (AVSF). Electron micrographs show that these large AVSF are lined with a layer of basal lamina on the inner surface of the limiting membrane and contain multilamellar bodies and electron-dense inclusions (Fig. 1). Furthermore, AVSF demonstrate closed spaces in serial sections [33], indicating that these structures must be generated independently of sarcolemmal indentation and that the inner AVSF compartment

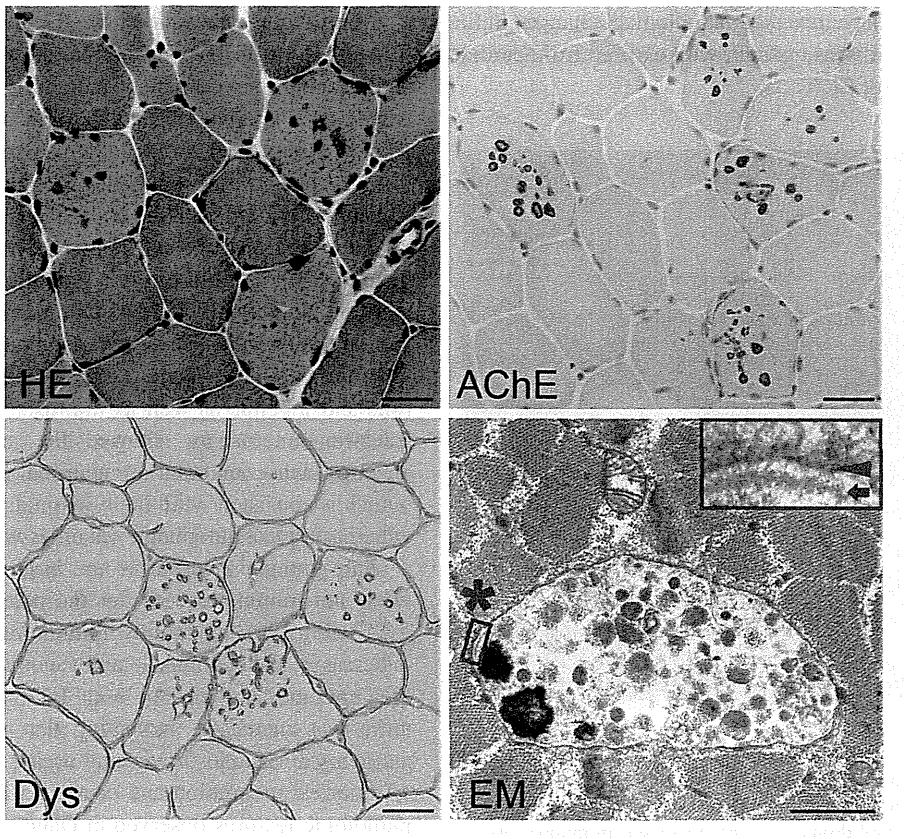

Fig. 1 Muscle pathology in Danon disease. Hematoxylin and eosin (HE)-stained sections show small *dot*-like basophilic granular structures in the muscle fibers, which are acetylcholine esterase (AChE)-positive autophagic vacuoles. The limiting membranes of autophagic vacuoles have sarcolemmal features, as demonstrated by immunohistochemistry using dystrophin antibodies (Dys). Electron microscopy (EM) confirms that these vacuoles have autophagic nature by revealing myeloid bodies, electron-dense granular material, and variable cytoplasmic debris; moreover, basal lamina is observed along the inner surface of an autophagic vacuole (*arrow* in the *inset*), providing further evidence that the vacuolar membrane has sarcolemmal features. The *inset* demonstrates the enlarged view of the area within the *square* marked with an *asterisk*. *Arrowhead* the membrane of the autophagic vacuole. *Scale bars* 50 μm (HE, AChE, and Dys) and 1 nm (EM)

should be topologically equivalent to the extracellular space. The mechanism by which this unique intracytoplasmic membrane structure is formed remains to be clarified; de novo generation is the most probable, supported by the observation that most AVSF are not accumulated in the subsarcolemmal region but are scattered in the cytoplasm without being connected to the sarcolemma. Furthermore, AVSF membrane, similar to neuromuscular junctions, demonstrates high activity of AChE. If AVSF were derived from sarcolemma, the AChE-expressing vacuoles should be located near neuromuscular junctions rather than scattered in the cytoplasm. Importantly, the frequency of AVSF occurrence increases with age and correlates with the progression of muscle weakness [33]. All these data indicate that AVSF formation, at least in the skeletal muscle, is a hallmark for the development of Danon disease [21, 22, 26, 27].

All Danon disease patients present severe cardiac symptoms, which include cardiomyopathy with or without arrhythmia and can lead to cardiac failure. Histological analysis reveals cardiomyocytes with dramatically increased vacuolation and clear degenerative features, including myofibrillar disruption and lipofuscin accumulation (Fig. 2). In addition, the immunoreactivity for microtubule-associated protein 1 light chain 3 (LC-3), a specific marker of autophagy, is increased in the autophagic vacuoles both in skeletal muscles and vacuolated cardiomyocytes.

Brain

Despite the presence of intellectual disability in the patients with Danon disease, very few neuropathological findings have been reported until recently. In an autopsy study,

Furuta et al. [13] have revealed pathological changes in the brain of a Danon disease patient who expired from cardiac failure at the age of 31.

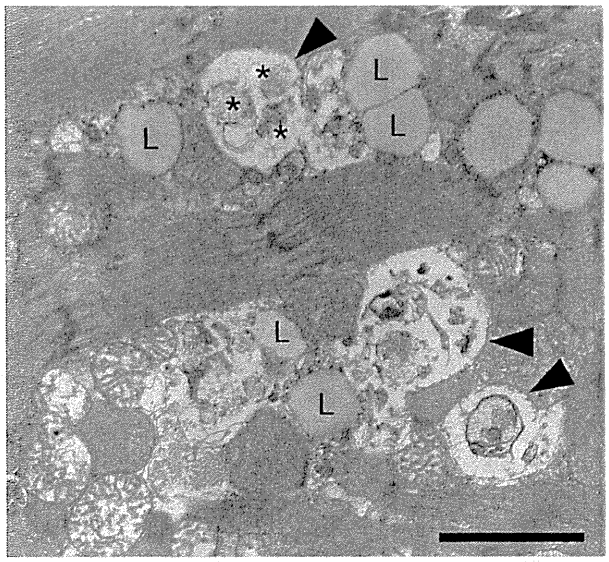

Fig. 2 Electron microscopy findings in the myocardium of Danon disease patients. Many vacuoles containing cytoplasmic debris (*asterisks*) are present. In addition, myofibrils are disorganized with mild Z-line streaming. Lipid droplets (L) are increased in number. *Arrow head* autophagic vacuoles; *scale bar* 1 μm

Microscopy analysis showed pale granular neurons found mainly in the nucleus basalis of Meynert (Fig. 3a) and cranial nerve nuclei, including oculomotor, dorsal vagal, and hypoglossal nuclei; some were detected in the frontal cortex. In addition, neurons containing lipofuscin-like granules were remarkably obvious, especially in the claustrum and inferior olivary nucleus, and the distribution of these neurons was different from that of pale granular neurons. The lipofuscin-like granules were positive for periodic acid–Schiff (PAS) staining, which detects glycogen and mucosubstances such as glycoproteins, and Luxol fast blue in Klüver–Barrera (KB) staining specific for neurons and myelins as well as lipofuscin granules (Fig. 3a). Electron microscopy showed the accumulation of the electron-dense material in neuronal perikarya (Fig. 3a), which is consistent with the lysosomal storage abnormality, whereas typical autophagic vacuoles were not observed.

Pale granular neurons in the basal nucleus of Meynert were not immunoreactive for the macroautophagy marker LC-3 (Fig. 3b) and faintly immunoreactive for ubiquitin, whereas in skeletal muscle and vacuolated cardiomyocytes, the immunoreactivity for both LC-3 (Fig. 3b) and ubiquitin was increased, indicating that the accumulation of autophagic vacuoles in visceral organs is enhanced because of retarded maturation and clearance. These tissue-specific pathologic features observed in Danon disease suggest that

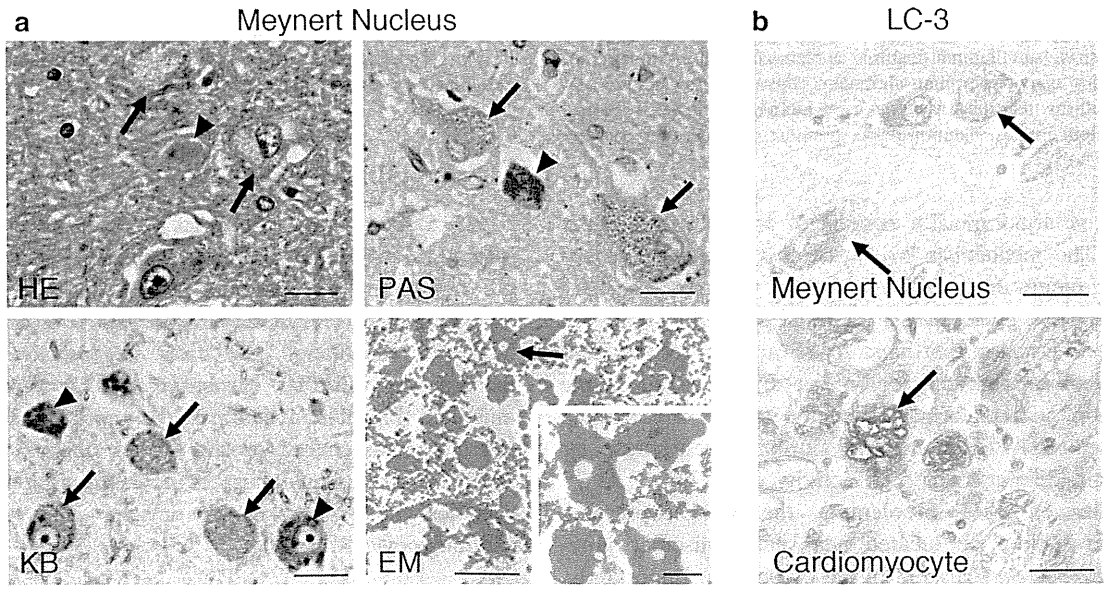

Fig. 3 Neuropathological findings in a Danon disease patient. **a** Pale granular neurons and neurons laden with lipofuscin-like granules (*arrows* and *arrowheads*, respectively, in HE, PAS, and KB) are seen in the basal nucleus of Meynert. *HE* hematoxylin–eosin, *PAS* periodic acid–Schiff, and *KB* Klüver–Barrera staining. Electron-dense material within small vacuoles is observed in the cytoplasm of the neurons in the basal nucleus (*arrow* in EM). **b** Pale granular neurons are scarcely immunoreactive for LC-3 (*arrows*, *upper panel*), whereas vacuolated cardiomyocytes are immunoreactive for LC-3 (*arrow*, *lower panel*). *Scale bars* 25 μm (HE, PAS, and KB, and b), 2 μm (EM), and 500 nm (EM, *inset*). This figure is modified from the original case report of Furuta et al. [13]

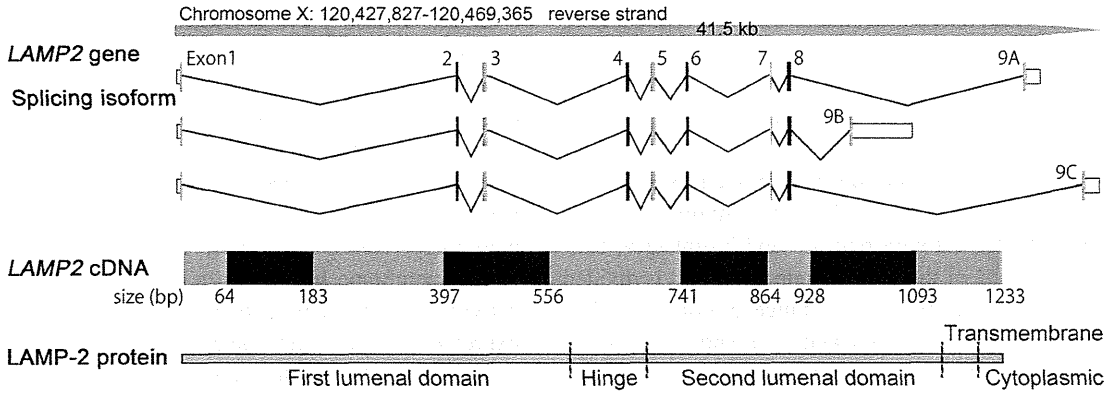

Fig. 4 Structure of the *LAMP2* gene. The open reading frame of the human *LAMP2* gene consists of 1,233 nucleotides and 9 exons encoding 410 amino acids. The three LAMP-2 splice isoforms, LAMP-2A, -2B, and -2C differ in the transmembrane and cytoplasmic domains encoded by the last exon 9 but have identical luminal domains

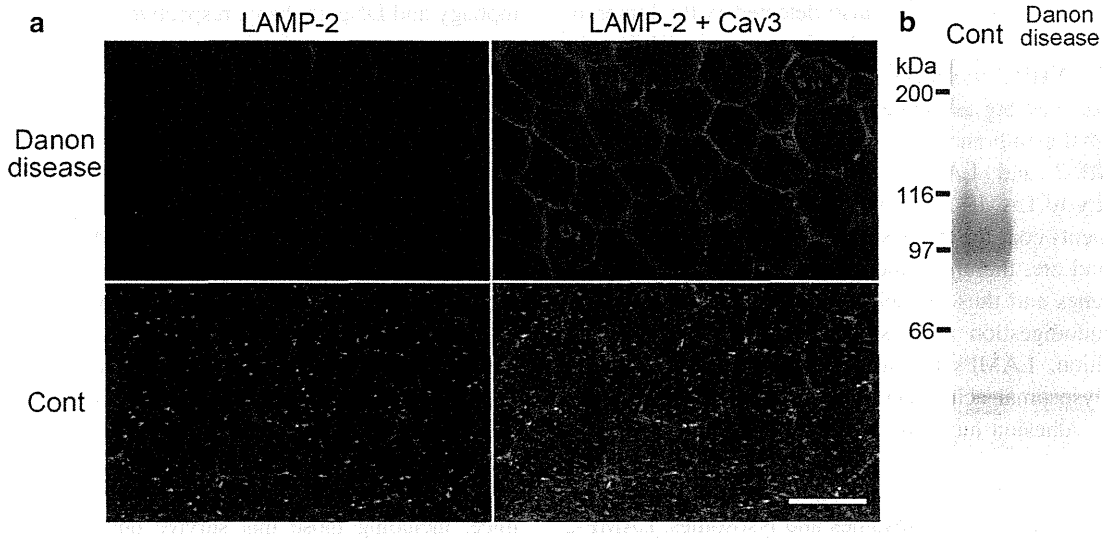

Fig. 5 LAMP-2 expression in skeletal muscles of a male patient with Danon disease. **a** Immunohistochemical staining with anti-LAMP-2 antibody shows that LAMP-2 expression is absent in skeletal muscles of a Danon disease patient, but present in those of an unaffected individual (Cont). The limiting membranes of autophagic vacuoles have sarcolemmal features, as demonstrated by staining with anti-caveolin-3 antibodies (LAMP-2 + Cav3). *Green* LAMP-2; *red* Cav3. *Scale bar* 50 μm. **b** Western blotting analysis of skeletal muscle extracts from a Danon patient and an unaffected individual using anti-LAMP-2 antibody. LAMP-2-deficiency in Danon disease is demonstrated

LAMP-2 in the brain may have functional properties distinct from those in the muscle.

Lamp-2

Gene structure

The open reading frame of the *LAMP2* gene consists of 1,233 nucleotides and encodes 410 amino acids (Fig. 4). The human *LAMP2* gene contains 9 exons; exons 1–8, and part of exon 9 encode the luminal domain; the rest of exon 9 encodes the transmembrane and cytoplasmic domains. Because of the alternative splicing of exon 9, there are three LAMP-2 isoforms, LAMP-2A, -2B, and -2C, which differ in the transmembrane and cytoplasmic domains but have identical luminal domains [5, 14, 16, 19].

Most of the mutations in the *LAMP2* gene currently identified in Danon disease lead to splicing defects or protein truncation, resulting in a loss of transmembrane and/or cytoplasmic domains, which underlies LAMP-2 protein deficiency, observed in cardiac and skeletal muscles, as